SUPPLEMENTAL MATERIAL

miRNA microarray assays: Primers for real-time qPCR

Eln_mus_120F GCGGACTTCCTGGTGGAGTTC

Eln_mus_269R CTCCAGGACCTGCTCCAAACG

Col1a1_mus_4184F GCGTAGCCTACATGGACCAG

Col1a1_mus_4330R AAGTTCCGGTGTGACTCGTG

Mcl1_mus_932F AGCTTCATCGAACCATTAGCAG

Mcl1_mus_1025R CAAACCCATCCCAGCCTCTTTG

Pparg_mus_1057F mouse AGCCTGCGGAAGCCCTTTGG

Pparg_mus_1197R mouse CAGCAAGCCTGGGCGGTCTC

Sirt3_mus_305F mouse TGGTTGAAGCCCACGGGACC

Sirt3_mus_407R mouse GGCACCCTGTCCGCCATCAC

CD36_mus_4F mouse GGCTGTGATCGGAACTGTGGGC

CD36_mus_98R mouse AGCATGTCTCCGACTGGCATGAG

Ppargc1a_mus_84F GTGTGTCAGAGTGGATTGGAG

Ppargc1a_mus_197R GAGCAGCACACTCTATGTCAC

The gene HPRT was used to normalize expression. Murine HPRT primer sequences:

Hprt_mus_147F TGCTCGAGATGTCATGAAGGAG

Hprt_mus_249R TTTAATGTAATCCAGCAGGTCAGC

Verification of miR-29 direct targets

The prediction of miRNA targets using bioinformatics algorithms has high false positive and false negative prediction rates.[39] Though false positive prediction can be excluded by experiments, false negative predictions would miss true targets. To further explore miR-29 potential direct targets, we employed a direct affinity purification method using a miRNA pull-down assay followed by specific quantitative PCR using established protocols.[40-42] In this approach, synthetic miRNA duplexes carrying a biotin group attached to the 3' end of the miRNA sense strand were transfected into murine PVSMCs. This resulted in the sense strand's subsequent incorporation into the miRNA-induced silencing complex (miRISC). After cell lysis, the miRNA-mRNA complexes were captured on streptavidin beads from which the mRNA was purified and analyzed using quantitative RT-PCR analysis of the affinity purified mRNA. The genes PPARγ, CD36, and CAV1 were evaluated as genes of interest suspected to be directly bound by miR-29. Elastin, and ABHD5 are known targets of miR-29 previously demonstrated, and used as positive controls; in contrast, G6PC and HPRT were used as negative controls with regard to miR-29 direct targeting.[43, 44]

Affinity purification of miR-29 direct targets

The sense strand of miRNA was labeled with biotin at 3'UTR end. The sense and the guide strand was synthesized separately and was annealed to form miRNA duplex. Synthesize Biotin-labeled miR-29a, b, c, scrambled microRNA sense strand or un-labeled guide strand as follows:

miR-29a-Bio:

uagcaccaucugaaaucgguuauu-Biotin

miR-29a:

uaaccgauuucagauggucggaag

miR-29b-Bio:

uagcaccauuugaaaucaguguu-Biotin

miR-29b:

cacugauuucaaauggugccaga

miR-29c-Bio:

uagcaccauuugaaaucgguuauu-Biotin

miR-29c:

uaaccgauuucaaauggugccag

Scrambled-Bio:

auuacgugaucuguuauaccacga-Biotin

Scrambled:

gugguauaacagaucucguaauag

Preparation of miRNA duplex and transfection

The miRNA sense and guide strand were annealed in 10 mM Tris, pH 7.5, 20 mM NaCl. The mixture was incubated for 2 minutes at 95° and then allowed to cool to room temperature on workbench for 2 hours. The miRNA duplex was transfected into murine

pulmonary smooth muscle cells at miRNA concentrations of 50 nM with lipofectamine 2000 (Invitrogen, Carlsbad, CA) according to the manufacturer's instructions.

Streptavidin purification of miRNA targets

Streptavidin purification of miRNA targets was performed according to the literature (PMID: 17889804). After purification, RNA was precipitated and dissolved in 20 µl of RNase-free water. All of the RNA was processed to cDNA with QuantiTect Reverse Transcription kit (Qiagen, Valencia, CA).

Supplemental Figure 1: miR-29 does not bind to the 3'UTR of the CD36 gene.

miR29 probes produced a product at cycle numbers comparable to that in scrambled probe, and in which melt curves, above, were characteristic of non-specific products. Specific products will have well-defined melt temperatures, as is the case for PPARγ in the figure above, which melts between 81 and 85 degrees C (black lines for triplicate products). By contrast, CD36 had no well defined melt temperature (grey lines), suggesting non-specific product or primer-dimers.

Supplemental Figure 2: Kidney histology

Mice exposed to α-miR29 treatment had no evidence of renal fibrosis upon histologic examination. In addition, there were no detectable abnormalities in terms of the renal glomeruli, tubules, or vasculature. Magnification, 20x.

Supplemental Figure 3: α-miR29 treatment increases average mitochondrial size

(A) Apparent mitochondrial long axis size is dependent on orientation of the mitochondria with respect to the cutting plane. For instance, a 500 nM mitochondria at a 60° angle to the cutting plane will have an apparent length of only 185 nM. **(B)** Assuming a random orientation, a 500 nM mitochondria will have a distribution of apparent sizes as depicted. **(C)** Distribution of measured sizes (symbols) is strong fit to distribution of expected sizes based on actual sizes as depicted in Figure 7A. **(D)** Measured sizes used to determine measurements of mitochondrial sizes in endothelial-like cells differentiated from iPS cells derived from human healthy controls shown in Figure 7D. **(E)** Measured

sizes used to determine measurements of mitochondrial sizes in endothelial-like cells differentiated from iPS cells derived from a BMPR2 mutant HPAH shown in Figure 7E.

Supplemental Figure 1

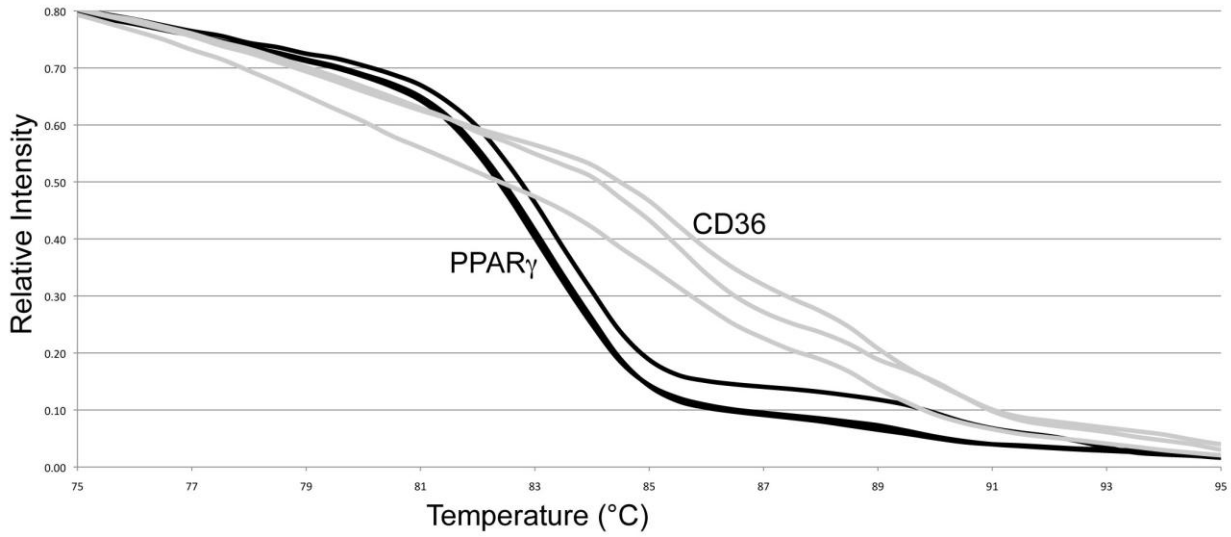

Supplemental Figure 2

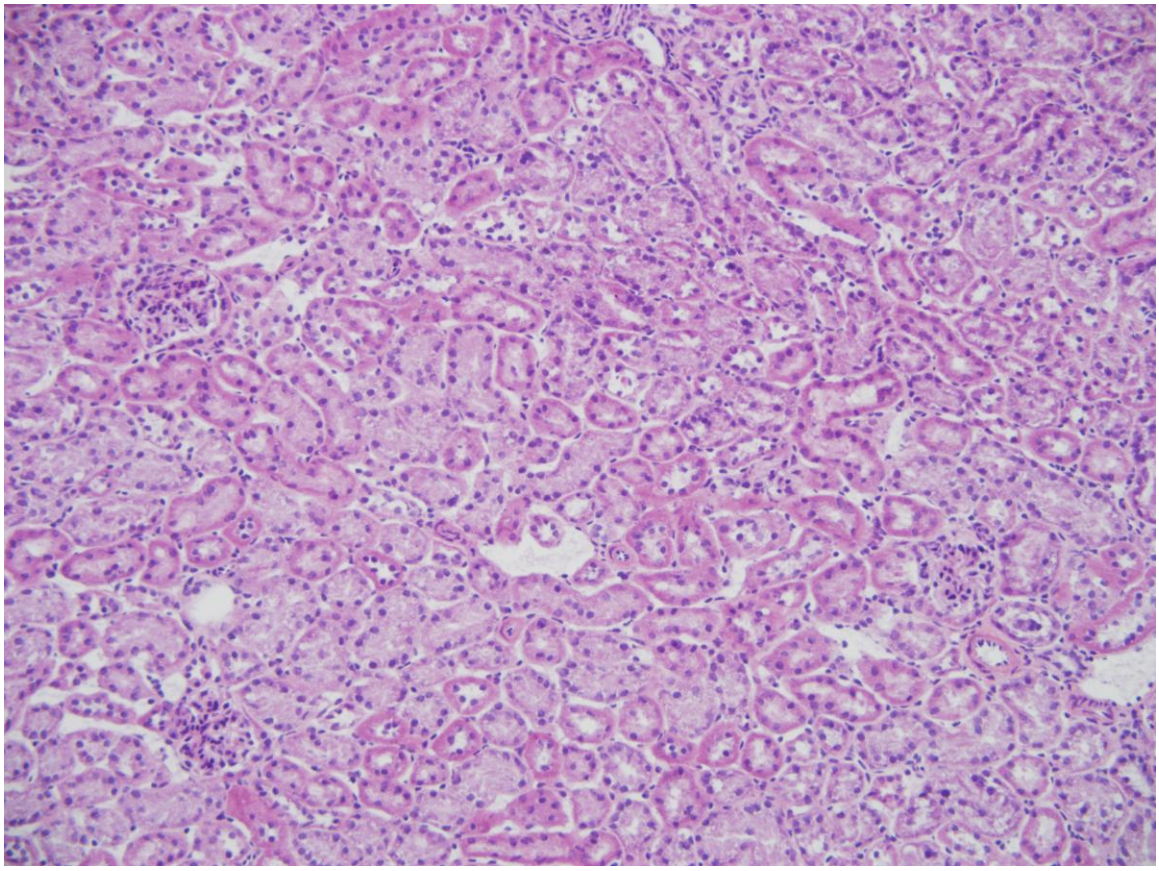

Supplemental Figure 3